Molecular Pharmacology Fast Forward. Published on November 13, 2012 as doi:10.1124/mol.112.082578

MOL #82578

Obtusilactone B from *Machilus thunbergii* targets barrier-to-autointegration factor to treat cancer

Wanil Kim, Ha-Na Lyu, Hyun-Sook Kwon, Ye Seul Kim, Kyung-Ha Lee, Do-Yeon Kim, Goutam Chakraborty, Kwan Yong Choi, Ho Sup Yoon, Kyong-Tai Kim

Department of Life Science, Division of Molecular and Life Science, Pohang University of Science and Technology, Pohang 790-784, Republic of Korea (W.K., H.-N.L., H.-S.K., Y.S.K., K.-H.L., D.-Y.K., K.Y.C., K.-T.K.); School of Biological Sciences, Nanyang Technological University, Singapore 637551 (G.C., H.S.Y.); Division of Integrative Biosciences and Biotechnology, Pohang University of Science and Technology, Pohang, 790-784, Republic of Korea (K.-T.K.)

Molecular Pharmacology Fast Forward. Published on November 13, 2012 as DOI: 10.1124/mol.112.082578
This article has not been copyedited and formatted. The final version may differ from this version.

Running title:

Obtusilactone B targets nuclear envelope dynamics

Corresponding author information:

Kyong Tai Kim, Ph.D, Professor

Laboratory of molecular neurophysiology, Department of Life Science, POSTECH

Hyojadong, Pohang, Kyungbuk, Korea 790-784

Tel: 82-54-279-2297

E-mail: ktk@postech.ac.kr

The number of text pages: 29

The number of tables: 1

The number of figures: 6

The number of references: 32

The number of words in abstract: 197

The number of words in introduction: 683

The number of words in discussion: 647

List of nonstandard abbreviations

BAF: barrier-to-autointegration factor

VRK1: *vaccinia*-related kinase 1

GST: glutathione-S-transferase

EGFP: enhanced green fluorescent protein

SPR: surface plasmon resonance

Molecular Pharmacology Fast Forward. Published on November 13, 2012 as DOI: 10.1124/mol.112.082578
This article has not been copyedited and formatted. The final version may differ from this version.

Abstract

Targeting specific molecules is a promising cancer treatment because certain types of cancer cells are dependent on specific oncogenes. This strategy led to the development of therapeutics that employ monoclonal antibodies or small molecule inhibitors. However, the continued development of novel molecular targeting inhibitors is required to target the various oncogenes associated with the diverse types and stages of cancer. Obtusilactone B is a butanolide derivative purified from *Machilus thunbergii*. Here, we show that obtusilactone B functions as a small molecule inhibitor, that causes abnormal nuclear envelope dynamics and inhibits growth by suppressing *vaccinia*-related kinase 1 (VRK1)-mediated phosphorylation of barrier-to-autointegration factor (BAF). BAF is important in maintaining lamin integrity, which is closely associated with diseases that include cancer. Specific binding of obtusilactone B to BAF suppressed VRK1-mediated BAF phosphorylation and the subsequent dissociation of the nuclear envelope from DNA that allows cells to progress through the cell cycle. Obtusilactone B potently induced tumor cell death *in vitro*, indicating that specific targeting of BAF to block cell cycle progression can be an effective anti-cancer strategy. Our results demonstrate that targeting a major constituent of the nuclear envelope may be a novel and promising alternative approach to cancer treatment.

Molecular Pharmacology Fast Forward. Published on November 13, 2012 as DOI: 10.1124/mol.112.082578
This article has not been copyedited and formatted. The final version may differ from this version.

Introduction

Targeted cancer therapy and personalized cancer therapeutics are aimed at a particular protein or even its polymorphic subtypes rather than common cellular factors shared by all proliferating cell types. This strategy is now anticipated to be effective against many kinds of tumors. In light of targeted cancer therapy concepts, determining the appropriate candidate oncogene to target with small molecules or monoclonal antibodies is very important. To date, most drugs in this category have been developed against oncogenic receptor tyrosine kinases or mitotic cellular kinases.

Because the rapid proliferation associated with the mutation of various growth factor receptors is an obvious cause of cancer, much effort has been spent developing drugs against these receptors. However, cell cycle-related proteins have recently drawn great attention from many researchers. Compared with extracellular growth factor receptors or secreted proteins, cell cycle-related intracellular factors play more fundamental and initiating roles, and therefore, can be more reliably targeted for drug development than traditional target proteins. For example, polo-like kinase 1 and aurora kinase B are involved in colorectal and lung cancers respectively, and have been added to the list of best target candidates for drug development (Lapenna and Giordano, 2009).

Here, we describe a kinase essential to normal mitosis, *vaccinia*-related kinase 1 (VRK1), which is highly expressed in fetal and cancerous tissues (Nezu et al., 1997). VRK1 plays a major role in cell cycle progression by phosphorylating histone H3 and barrier-to-autointegration factor **(**BAF), leading to chromatin condensation and nuclear envelope breakdown respectively (Kang et al., 2007; Nichols et al., 2006). VRK1-mediated BAF phosphorylation is one of the most important events in both mitosis and meiosis (Lancaster et al., 2007; Nichols et al., 2006). BAF is highly conserved and is important in the regulation of

Molecular Pharmacology Fast Forward. Published on November 13, 2012 as DOI: 10.1124/mol.112.082578
This article has not been copyedited and formatted. The final version may differ from this version.

nuclear architecture (Margalit et al., 2007; Skoko et al., 2009). During the resting G0 phase, a complex of genomic chromatin and BAF is tethered to the nuclear envelope by various nuclear membrane protein complexes that contain lamina-associated polypeptide 2/emerin/Man1 domains (Furukawa et al., 2003). This link between chromatin and the nuclear envelope must be disrupted to allow the cell to cycle from G0 into S phase and into the subsequent G2/M phase. Once the link is disrupted, VRK1 phosphorylates BAF (Lancaster et al., 2007; Nichols et al., 2006), and the phosphorylated BAF releases DNA from the nuclear envelope; this release is followed by DNA synthesis, transcription factor binding, and DNA condensation (Haraguchi et al., 2007; Lancaster et al., 2007; Margalit et al., 2007). Furthermore, VRK1 is also involved in the G1/S transition and the entry into mitosis (Kang et al., 2008; Lopez-Sanchez et al., 2009; Valbuena et al., 2008). Because of their prominent roles in tumorigenesis, we proposed the oncogene VRK1 and its cognate substrate BAF as novel targets of molecular medicine and thus initiated a search for small molecule inhibitors of VRK1 and BAF.

We acquired a natural herb library in which to search for small molecule inhibitors of VRK1. This system has certain merits compared to synthetic or inorganic libraries. Natural products have played a significant role in drug discovery and specifically in the development of new anti-cancer agents; more than 79.8% of the anti-cancer drugs introduced from 1981 to 2008 were natural products, semisynthetic analogues, or synthetic compounds based on natural-product pharmacophores (Cragg et al., 2009).

To find inhibitory molecules of VRK1, we performed high through-put screening of compounds derived from *Machilus thunbergii* Sieb. et Zucc. (Lauraceae), a deciduous tree of Korea and Japan. *M. thunbergii* has long been used as a traditional medicine in Korea, China and Japan to treat various diseases including edema, abdominal pain, and abdominal

Molecular Pharmacology Fast Forward. Published on November 13, 2012 as DOI: 10.1124/mol.112.082578
This article has not been copyedited and formatted. The final version may differ from this version.

distension. Next, we characterized four butanolide derivatives whose hexane subfractions prominently inhibited the phosphorylation of BAF by VRK1. Further characterization by surface plasmon resonance (SPR) detection and nuclear magnetic resonance titration of the most promising VRK1 inhibitor, obtusilactone B, demonstrated that the inhibitor specifically bound the substrate BAF. This interaction suppressed the phosphorylation of BAF by VRK1, thus arresting the cell cycle by causing defective mitotic nuclear envelope dynamics. We also showed preferential cytotoxicity of obtusilactone B toward tumor cells via cell viability assays.

Molecular Pharmacology Fast Forward. Published on November 13, 2012 as DOI: 10.1124/mol.112.082578
This article has not been copyedited and formatted. The final version may differ from this version.

Materials and Methods

NMR titration of recombinant BAF with inhibitors.

Binding modes of the small molecule BAF inhibitors were examined by studying the 2D ^{1}H, ^{15}N-Heteronuclear Single Quantum Correlation Spectroscopy (HSQC) spectrum of recombinant BAF protein before and after addition of the inhibitors. For this, the recombinant BAF protein was uniformly labeled using ^{15}N-ammonium chloride and purified according to previously described protocol (Cai et al., 1998). HSQC spectrum of BAF was recorded using 0.3 mM protein sample on a Bruker Avance 700 spectrometer at 298 K. Ligands were then added to the sample and the chemical shifts were compared before and after the addition of the ligand. A plot of average chemical perturbations versus the amino acids was studied according to the previously described method (Chakraborty et al., 2012).

Protein Ligand Docking studies

GOLD 5.0 (Genetic Optimization for Ligand Docking, Cambridge Crystallographic Data Centre, UK) program (Verdonk et al., 2003) was used for docking studies. The crystal structure BAF protein in complex with DNA (PDB 2BZF) (Bradley et al., 2005) was prepared for docking studies by deleting the heteroatoms; assigning the charges and potentials by CHARM force field and energy minimized with conjugate gradients algorithm in Discovery Studio (DS) 3.1 (Accelrys, 2011). The ligands compound #**1** & compound #**3** were built with 3D-sketcher and energy minimized with smart minimizer algorithm module in DS 3.1 and thus minimized molecules were used for docking studies. An active site radius of 10.0 Å around DNA binding region of BAF was used to define the active site point and default docking parameters were employed to dock the compound #**1**, compound #**3** into the DNA binding site of BAF.

Molecular Pharmacology Fast Forward. Published on November 13, 2012 as DOI: 10.1124/mol.112.082578
This article has not been copyedited and formatted. The final version may differ from this version.

Plant Material and Purified Compound Identification.

The stems of *Machilus thungergii* were purchased from an oriental drug store in Pohang, Gyeongbuk, Korea, in July 2009. Plant material was identified by Yong-Ki Park (Department of Herbalogy, College of Oriental Medicine, Dongguk University, Gyeongju, Korea). A voucher specimen (MT2009-01) is reserved at the Laboratory of Molecular Neurophysiology, POSTECH, Pohang, Korea. Optical rotation was measured on a JASCO P-1020 polarimeter. The infra-red (IR) spectrum was obtained with a Perkin-Elmer Spectrum GX FT-IR spectrometer. EI-MS spectra were obtained with a WATERS Micromass Platform II mass spectrometer or Agilent 7890A-5975C GC/MSD. ^{1}H-NMR, ^{13}C-NMR, DEPT, COSY, HMBC and HMQC NMR spectra were recorded on a Bruker DRX-500 FT-NMR spectrometer and a Bruker Avance 700 spectrometer. Chloroform-d_1 with TMS as internal standard was purchased from Sigma (St. Louis, MO, USA). Merck Silica gel 60 (63~200 μm) and LiChroperp RP-18 (40~63 μm) were used for column chromatography. Analytical TLC was performed on Merck Silica gel 60 F-254 and Silica gel 60 RP-18 F-254 TLC plates. Spots were detected by UV light (254 and 365 nm) and spraying with 10% H_2SO_4 and then heating on a hot plate.

NMR Characterization of Natural Compounds

Componds **#1**~**#4** were characterized by comparison of their spectroscopic data including NMR, MS and IR with literature values (Anderson et al., 1992; Hiroyuki Karikome, 1991; Kuo et al., 2008; Masatake Niwa, 1975).

Obtusilactone B (#1): yellowish oil. IR (KBr, cm^{-1}): 3575, 3000, 1790, 1685; EI/MS m/z : 335 $[M+H]^+$, 334$[M]^+$, 317$[M+H-H2O]^+$, 291$[M-43]^+$, 179, 177, 140, 135, 126, 123, 109,

Molecular Pharmacology Fast Forward. Published on November 13, 2012 as DOI: 10.1124/mol.112.082578
This article has not been copyedited and formatted. The final version may differ from this version.

97, 95, 83, 81, 79, 70, 69, 67, 57, 55, 43, 41; ^{1}H-NMR (500 MHz, $CDCl_3$, δ): 6.69 (1H, td, *J*=8.0, 2.0 Hz, H-1'), 5.35(2H, m, H-7', 8'), 5.12 (1H, br s, H-4), 4.89 (1H, dd, *J*=3.5, 2.0 Hz, H-6b), 4.68 (1H, dd, *J*=3.0, 1.0 Hz, H-6a), 2.78 (2H, m, H-2'), 2.03 (2H, m, H-6'), 2.03 (2H, m, H-9'), 1.50 (2H, qui, *J*=7.0 Hz, H-3'), 0.90 (3H, br t, *J*=7.0 Hz, H-16'); ^{13}C-NMR (125 MHz, $CDCl_3$, δ): 165.3 (C-2), 157.6 (C-5), 151.2 (C-1'), 130.2 (C-8'), 129.4 (C-7'), 126.9 (C-3), 90.2 (C-6), 68.8 (C-4), 31.9 (C-14'), 29.8~28.9 (C-4',5',10'~13'), 28.6 (C-2'), 28.3 (C-3'), 27.2 (C-9'), 27.0 (C-6'), 22.7 (C-15'), 14.1 (C-16').

Secosubamolide A (#2): pale yellowish liquid. IR (KBr, cm^{-1}): 3450, 1735, 1710; EI/MS m/z : 369 $[M+H]^+$, 351$[M+H-H2O]^+$, 325$[M-43]^+$, 293, 265, 247, 191, 149, 125, 115, 97, 83, 69, 55; ^{1}H-NMR (500 MHz, $CDCl_3$, δ): 7.09 (1H, t, *J*=7.5 Hz, H-3), 4.92 (1H, br s, H-1'), 3.75 (3H, s, OMe), 2.38 (2H, q, *J*=7.5 Hz, H-4), 2.17 (3H, s, H-3'), 1.53 (2H, qui, *J*=7.5 Hz, H-5), 0.90 (3H, br t, *J*=7.0 Hz, H-18); ^{13}C-NMR (125 MHz, $CDCl_3$, δ): 206.3 (C-2'), 166.5 (C-1), 149.1 (C-3), 129.7 (C-2), 73.4 (C-1'), 52.0 (OMe), 31.9 (C-16), 29.7~29.3 (C-6~15), 28.7 (C-5), 28.7 (C-4), 24.8 (C-3'), 22.7 (C-17), 14.1 (C-18).

2-Octadecylidene-3-hydroxy-4-methylenebutanolide (#3): solid. IR (KBr, cm^{-1}): 3584, 3350, 3020, 2935, 2860, 1780, 1680, 1665, 1465, 1270, 1205, 1145, 1060, 1015, 950, 860, 830, 815; EI/MS m/z : 365 $[M+H]^+$, 364$[M]^+$, 347$[M+H-H2O]^+$, 321$[M-43]^+$, 140, 135, 126, 123, 109, 97, 95, 83, 81, 79, 70, 69, 67, 57, 55, 43, 41; ^{1}H-NMR (500 MHz, $CDCl_3$, δ): 7.05 (1H, td, *J*=8.0, 2.0 Hz, H-1'), 5.22 (1H, br d, H-4), 4.93 (1H, dd, *J*=3.0, 2.0 Hz, H-6b), 4.70 (1H, dd, *J*=3.0, 1.0 Hz, H-6a), 2.45 (2H, m, H-2'), 1.52 (2H, qui, *J*=7.5 Hz, H-3'), 0.88 (3H, br t, *J*=7.0 Hz, H-18'); ^{13}C-NMR (125 MHz, $CDCl_3$, δ): 166.8 (C-2), 157.7 (C-5), 150.1 (C-1'), 127.4 (C-3), 91.2 (C-6), 66.4 (C-4), 31.9 (C-16'), 29.7~29.4 (C-2', 4'~15'), 28.3 (C-3'), 22.7 (C-17'), 14.1 (C-18').

Linderanolide (#4): crystals. IR (KBr, cm^{-1}): 3395, 2920, 2850, 1779, 1770, 1671, 1469,

Molecular Pharmacology Fast Forward. Published on November 13, 2012 as DOI: 10.1124/mol.112.082578
This article has not been copyedited and formatted. The final version may differ from this version.

1275, 1033, 948, 863, 718; EI/MS *m/z* : 337 $[M+H]^+$, 336$[M]^+$, 319$[M+H-H_2O]^+$, 293[M-43]$^+$, 140, 135, 126, 123, 109, 97, 95, 83, 81, 79, 70, 69, 67, 57, 55, 43, 41; ^{1}H-NMR (500 MHz, $CDCl_3$, δ): 6.69 (1H, td, *J*=8.0, 2.0 Hz, H-1'), 5.12 (1H, br d, H-4), 4.89 (1H, dd, *J*=3.0, 2.0 Hz, H-6b), 4.68 (1H, dd, *J*=3.0, 1.0 Hz, H-6a), 2.78 (2H, m, H-2'), 1.49 (2H, qui, *J*=7.0 Hz, H-3'), 0.89 (3H, br t, *J*=7.0 Hz, H-16'); ^{13}C-NMR (125 MHz, $CDCl_3$, δ): 165.2 (C-2), 157.6 (C-5), 151.3 (C-1'), 126.8 (C-3), 90.3 (C-6), 68.9 (C-4), 31.9 (C-14'), 29.7~29.3 (C-4'~13'), 28.7 (C-2'), 28.3 (C-3'), 22.7 (C-15'), 14.1 (C-16').

Extraction and Isolation

The dried stems of *Machilus thunbergii* (20 kg) were extracted with *n*-hexane (40 L × 2) at room temperature. The extract was obtained by concentration under reduced pressure. The *n*-hexane extract (50 g among a total of 151 g) was chromatographed over silica gel (70-230 mesh, 7.5× 12 cm) and eluted with a gradient of *n*-haxane-EtOAc (6:1, 4:1, 2:1, and 1:1) and acetone to produce eleven fractions (MTH1~MTH11). Fraction MTH5+6 (5.35 g) was subjected to a silica gel column chromatography (4.5×15 cm), eluted with *n*-hexane-EtOAc (7:1) to obtain 11 fractions (MTH5+6-1~MTH5+6-11). Fraction MTH5+6-4+5 (1.75 g) was purified by an octadecyl silica gel (ODS) column chromatography (4×5 cm) and eluted with MeOH -H_2O (13:1) to ultimately produce compound **3** (80.0 mg). Fraction MTH7+8 (1.7 g) was subjected to a silica gel column chromatography (4.5×15 cm), eluted with $CHCl_3$-acetone (100:1) to obtain 11 fractions (MTH7+8-1~MTH7+8-11). Fraction MTH7+8-4 (1.3 g) was applied to an ODS column chromatography (4×6 cm) and eluted with MeOH -H_2O (9:1, 10:1 and 12:1) to produce compound **1** (50 mg), compound **2** (31 mg) and compound **4** (35 mg).

Molecular Pharmacology Fast Forward. Published on November 13, 2012 as DOI: 10.1124/mol.112.082578
This article has not been copyedited and formatted. The final version may differ from this version.

Cell culture, Transfection and Flow Cytometry

A549 cell was cultured in RPMI-1640 medium (Welgene, Korea) containing 10% of fetal bovine serum (Hyclone, USA) and 1% penicillin/streptomycin (Welgene, Korea) in a humidified 5% CO_2 incubator at 37^{o}C. B16F-10 cell was fed in DMEM medium. Transient transfection was performed by a microporator MP-100 (Invitrogen, USA) according to manufacturer's instruction (1300V, 20ms, #2). For flow cytometric analysis, cells were fixed with 70% ethanol containing 0.4% Tween-20. Cellular DNA was stained with 50μg/ml of proppidium iodide (Fluka, USA) and 100μg/ml of RNase A (Sigma, USA) in PBS. Sample containing 5,000 cells were analyzed on a FACSCalibur system (BD, USA).

Plasmids, Antibody, Recombinant Protein Purification and in vitro Kinase Assay

To generate barrier-to-autointegration factor (BAF) expression construct, full-length BAF was amplified by PCR from HeLa cells. For mammalian expression, DNA fragment coding for BAF was cloned into pEGFP-C1 (Clontech Laboratories, USA). GST-tagged VRK1 and histidine-tagged BAF were prepared as previously described (Harris and Engelman, 2000; Kang et al., 2008). For red fluorescent protein-tagged VRK1, DNA fragment coding for VRK1 was cloned into pDsRed-Monomer-N1 (Clontech Laboratories, USA). *In vitro* kinase assay between recombinant VRK1 and BAF was performed as previously described(Kim et al., 2011). Antibody against Lamin A/C (N-18) was purchased from Santa Cruz.

Surface Plasmon Resonance (SPR)

The interaction between the BAF and obtusilactone B was analyzed by SPR, using the Reichert SR7500DC system (Reichert Technologies, USA) and data collection software (SPR Autolink v1.1.8G). BAF protein, the ligand, was covalently bound to carboxymethyl dextran

Molecular Pharmacology Fast Forward. Published on November 13, 2012 as DOI: 10.1124/mol.112.082578
This article has not been copyedited and formatted. The final version may differ from this version.

sensor chip (CMDH gold slide) with 1-ethyl-3(3-dimethylaminopropyl) carbodiimide-HCl (EDC) and *N*-hydroxysuccinimide (NHS). The ligand was bound at densities about 2400 RU, where RU, resonance units, 1RU = 1pg/mm^2 on the sensor surface. Obtusilactone B and 2-octadecylidene-3-hydroxy-4-methylenebutanolide, the analytes, were injected over the sensor surface at the indicated concentrations diluted in 10mM phosphate-buffered saline containing 1% of DMSO. RUs were recorded in real time before and during small molecule injection (1 minute) and during washout (2 minutes). Analysis of steady-state affinity was performed using Scrubber2 software selecting reference-subtracted curves. Recorded responses that included disturbances produced by air bubbles, aggregation, or precipitation of analytes were discarded. In the global approach all the samples, including both association and dissociation steps, are fit at the same time using a sum of squared residuals over every data point.

Dye Conjugation

Obtusilactone B was covalently conjugated with a red fluorescent dye, FPR552 (Bioacts, Korea – λ abs : 551nm, λ em : 570nm). Ethanol-solubilized obtusilactone B and FPR552 were reacted in dimethylformamide and then 0.1M phosphate buffer (pH 12.0) was added. After 4 hours of incubation at room temperature, the FPR552-obtusilactone B conjugates were lyophilzed and purified under Agilent 1100 series HPLC system using Jupiter 10u C18 300A 250X10mm column.

Cell Viability Assay

Cell viability was assessed by measuring the activity of metabolizing 3-(4,5-dimethyldiazol-2-yl)-2,5-diphenyltetrazolium bromide (MTT) (Choi et al., 2008). 1.0 x 10^4 cells were seeded onto 96-well plate and cultured up to confluency of 90%. After treating indicated

Molecular Pharmacology Fast Forward. Published on November 13, 2012 as DOI: 10.1124/mol.112.082578
This article has not been copyedited and formatted. The final version may differ from this version.

concentration of inhibitors for 24 hours, cells were treated with MTT solution and cell viability was assessed.

Molecular Pharmacology Fast Forward. Published on November 13, 2012 as DOI: 10.1124/mol.112.082578
This article has not been copyedited and formatted. The final version may differ from this version.

Results

Small molecule inhibitors of BAF phosphorylation

To find small molecule inhibitors of VRK1, we analyzed hundreds of natural herb extracts prepared by extraction of Korean traditional herbs in 80% methanol (Supplemental Figure 1). Among them, the crude extract of *M. thunbergii* substantially inhibited the autophosphorylation of VRK1. We next conducted *in vitro* kinase assays with *M. thunbergii* to find inhibitory molecules against VRK1 action by performing solvent-based extraction and purifying active sub-fractions (Fig. 1A). Certain fractions derived from hexane and butyl alcohol extraction completely inhibited the catalytic activity of VRK1 towards BAF. We further fractionated the hexane extract to purify the bioactive inhibitor molecule (Fig. 1B). We successfully isolated and characterized four bioactive butanolides: obtusilactone B (compound **#1**), secosubamolide A (compound **#2**), 2-octadecylidene-3-hydroxy-4-methylenebutanolide (compound **#3**), and linderanolide (compound **#4**). This study describes the first isolation of compounds **#1**, **#2**, and **#4** from *M. thunbergii* (Fig. 1C).

Obtusilactone B suppresses VRK1-mediated phosphorylation of BAF

VRK1 is a cell cycle-regulating protein kinase and acts on several related substrates that include p53, histone H3, BAF, and CREB (Kang et al., 2007; Kang et al., 2008; Nichols et al., 2006; Valbuena et al., 2008). Because BAF is one of the most important substrates of VRK during mitosis, during which BAF phosphorylation is required for DNA condensation and mitotic progression (Suzuki et al., 2010; Vlcek et al., 2001), we primarily analyzed whether our novel butanolide derivatives suppressed the enzymatic reaction of VRK1 toward BAF (Fig. 2A). Although two derivatives inhibited BAF phosphorylation, inhibition by obtusilactone B (compound **#1**) was the most pronounced. We next serially diluted

Molecular Pharmacology Fast Forward. Published on November 13, 2012 as DOI: 10.1124/mol.112.082578
This article has not been copyedited and formatted. The final version may differ from this version.

obtusilactone B to estimate its median inhibitory concentration (Fig. 2B) and found that obtusilactone B strongly inhibited BAF phosphorylation by VRK1 *in vitro* with a median inhibitory concentration of 0.8 μM. Interestingly, obtusilactone B inhibited VRK1 auto-phosphorylation very little, indicating that rather than occupying the ATP-binding domain or another conserved domain as many kinase inhibitors do, obtusilactone B may inhibit the interaction between VRK1 and BAF. We next tested other VRK1 substrates to confirm the inhibitory activity observed. To our surprise, obtusilactone B did not inhibit the catalytic activity of VRK1 toward histone H3 or casein peptide (Fig. 2D and 2E) even though it inhibited BAF phosphorylation (Fig. 2C); this observation suggests that obtusilactone B specifically inhibits the interaction between VRK1 and BAF.

Obtusilactone B specifically interacts with BAF

To understand the molecular basis of the interaction between obtusilactone B and BAF suggested by the *in vitro* kinase assays, we studied the interaction between ^{15}N-labeled recombinant BAF and obtusilactone B by nuclear magnetic resonance spectroscopy (Fig. 3A). Chemical shift perturbations observed in the heteronuclear single quantum coherence spectrum of BAF upon addition of the ligands obtusilactone B and 2-octadecylidene-3-hydroxy-4-methylenebutanolide were analyzed and mapped on the surface of BAF (Fig. 3B). Obtusilactone B binds BAF strongly, as indicated by dramatic chemical shift perturbations observed upon the addition of the ligand to the protein. In contrast, the inactive ligand 2-octadecylidene-3-hydroxy-4-methylenebutanolide binds the protein weakly, as evidenced by smaller changes upon the addition even of high molar ratios of the inactive ligand (*e.g,*. 10:1 2-octadecylidene-3-hydroxy-4-methylenebutanolide : BAF, data not shown). The residues whose backbone amide resonance was dramatically affected by the obtusilactone B

Molecular Pharmacology Fast Forward. Published on November 13, 2012 as DOI: 10.1124/mol.112.082578
This article has not been copyedited and formatted. The final version may differ from this version.

interaction included S22, A24, K32, G31, and E35 (Fig. 3A). These residues are located near the protein's helix-loop-helix region, which plays a major role in its interaction with double stranded DNA molecules (Bradley et al., 2005). Other residues, such as D9, Q73, and D76, also exhibited chemical shift perturbations in our study. An overlay of the heteronuclear single quantum coherence spectrum of the free BAF protein and the bound protein (1:1 molar ratio obtusilactone B : BAF) is presented in Supplemental Figure 2.

In silico modeling and analysis of the binding mode of obtusilalactone B

Obtusilactone B clearly bound near the DNA binding site of BAF (Bradley et al., 2005). The hexadec-7-enylidene bond of the obtusilactone B molecule seems to interact favorably with the glycine-rich region of BAF, forming tight van der Waal contacts with residues G21, G25, G29, and G31. The 4-hydroxy-5-methylene-dihydro-furan-2-one moiety of obtusilactone B is stabilized by hydrogen bonding with residue E28 and hydrophobic interactions with residues V20, G25, I26, V29, L30, G31, and K32 in the hydrophobic groove (Fig. 3D). In contrast, the same moiety of 2-octadecylidene-3-hydroxy-4-methylenebutanolide fails to form these interactions and drifts away from the active pocket. The failure to interact with E28, the lack of unsaturated bonds, and a carbon chain lengthier by two atoms are probable reasons for the inactivity of 2-octadecylidene-3-hydroxy-4-methylenebutanolide (Fig. 3D). Taken together, our results suggest that obtusilactone B suppresses the VRK1-mediated phosphorylation of BAF specifically by binding near the DNA binding site of BAF. It is unclear whether this region is important in the interaction between VRK1 and BAF. However, the specific interaction between obtusilactone B and the N-terminal region of BAF, proximal to residues phosphorylated by VRK1 (Nichols et al., 2006), indicates the possible identification of obtusilactone B as a novel small molecule inhibitor that targets a major nuclear envelope

Molecular Pharmacology Fast Forward. Published on November 13, 2012 as DOI: 10.1124/mol.112.082578
This article has not been copyedited and formatted. The final version may differ from this version.

constituent.

SPR evidence for the interaction of obtusilactone B with BAF

The interaction between BAF and obtusilactone B was further evidenced by SPR analysis and cytochemistry with fluorescent dye-conjugated obtusilactone B. SPR employs various biosensor systems to detect molecular interactions (Karlsson et al., 1991). We immobilized the BAF protein to a gold sensor chip slide and applied obtusilactone B to the slide. Sensor chip-immobilized BAF protein was more sensitive to obtusilactone B than to 2-octadecylidene-3-hydroxy-4-methylenebutanolide (Fig. 4A). Calculated binding constants are presented in Table 1. As previous results suggest, obtusilactone B, the inhibitor of VRK1-mediated BAF phosphorylation, exhibited a higher binding affinity for BAF than did 2-octadecylidene-3-hydroxy-4-methylenebutanolide. Unreferenced raw data and responses of immobilized VRK1 protein are also presented in Supplemental Figure 3. These results suggest that obtusilactone B specifically binds to BAF, but does not bind VRK1.

Expression of enhanced green fluorescent protein-labeled BAF induced the localization of FPR552-conjugated obtusilactone B to the nucleus, to which native BAF protein localizes (Fig. 4B and 4C). In contrast, neither the unconjugated dye FPR552 nor enhanced green fluorescent protein co-localized with each other. Taken together, our data suggest that obtusilactone B, a small molecule inhibitor of BAF phosphorylation, specifically interacts with BAF near the protein's DNA binding region, thereby inhibiting BAF phosphorylation by VRK1.

Physiological perturbations induced by obtusilactone B treatment

As mentioned above, BAF plays an important role in nuclear envelope structure (Vlcek et

Molecular Pharmacology Fast Forward. Published on November 13, 2012 as DOI: 10.1124/mol.112.082578
This article has not been copyedited and formatted. The final version may differ from this version.

al., 2001). The interactions and dynamics of nuclear membrane proteins must be tightly coordinated during many cellular processes including cell cycle progression (Furukawa et al., 2003; Gorjanacz et al., 2007; Lancaster et al., 2007). Specifically, the interaction between chromatin and the nuclear envelope must be disrupted at the G1/S transition that occurs at the beginning of the cell cycle. At this stage, BAF is phosphorylated by VRK1, and next, chromatin is released from the nuclear envelope (Lancaster et al., 2007; Nichols et al., 2006). We visualized the mitotic nuclear envelope fragment by staining nuclear lamin A/C of A549 cells (Fig. 5A) and found that nuclear lamin A/C was dispersed into the cytosol at late anaphase. However, this release was completely abolished by treatment with obtusilactone B: compared with vehicle-treated cells, A549 cells grown in medium containing obtusilactone B could not release the nuclear envelope fragment containing lamin A/C from chromatids. This inability to release the fragment might be attributed to the inhibitory action of obtusilactone B on the phosphorylation of BAF by VRK1. To further analyze this cellular effect, we expressed VRK1 and BAF in concert with obtusilactone B treatment (Fig. 5B). As previously demonstrated (Nichols et al., 2006), co-expression of BAF and VRK1 induced their translocation into the cytosol, and this translocation was accompanied by DNA condensation. However, in obtusilactone B-treated cells, BAF could not translocate into the cytosol but was trapped by the contorted nucleus despite the presence of VRK1. These results indicate that obtusilactone B blocked BAF phosphorylation by VRK1, resulting in dysfunctional cellular processes. Because the phosphorylation of BAF is involved in cell cycle initiation, we quantitatively assessed the DNA content of obtusilactone B-treated cells by flow cytometry (Fig. 5C and 5D). The A549 cell population treated with obtusilactone B included a significantly increased number of cells in the G1 phase, which possibly resulted from the defective DNA release from the nuclear envelope during the G1/S transition and the

Molecular Pharmacology Fast Forward. Published on November 13, 2012 as DOI: 10.1124/mol.112.082578
This article has not been copyedited and formatted. The final version may differ from this version.

subsequent delay in cell cycle progression. This defect was successfully rescued by the introduction of GFP-tagged BAF protein suggesting that obtusilactone B-induced cell cycle arrest was induced by the silencing of endogenous BAF.

Anti-cancer activity of obtusilactone B

Because the suppression of BAF phosphorylation by VRK1 in obtusilactone B-treated cells appeared to trigger defective cell cycle progression, we next analyzed the anti-tumor activity of obtusilactone B. First, we performed a cell viability assay to provide evidence for the proposed molecular mechanism of interference with cell growth or viability. The obtusilactone B was moderately cytotoxic to A549 (Fig. 6A) and HeLa (Fig. 6B) cells. However, 2-octadecylidene-3-hydroxy-4-methylenebutanolide was significantly less cytotoxic than obtusilactone B. We assume that the difference in cytotoxicity is derived from the ability of obtusilactone B to specifically target endogenous proteins such as BAF.

We also analyzed the specificity of obtusilactone B against tumor cells versus normal cells. We prepared mouse embryonic fibroblast derived from the C57BL/6 strain as a normal cell control. B16F10, a metastatic melanoma fibroblast line derived from the C57BL/6 strain was prepared as the cancer cell control. As shown in Fig. 6C, obtusilactone B effectively killed metastatic melanoma cells. However, mouse embryonic fibroblast cells were quite resistant to obtusilactone B compared to melanoma cells. This result shows that obtusilactone B might target highly proliferative cancer cells with specificity. Obtusilactone B also effectively killed teratocarcinoma cells at very low concentrations approaching 1 μM (Fig. 6D).

The effect of obtusilactone B on aneuploidy was assessed by analyzing the molecule's effect on a cell population containing DNA content more than 4N (Fig. 6E and 6F). Treatment with 10 μM obtusilactone B for 72 hours effectively induced cell death in the aneuploid cell

Molecular Pharmacology Fast Forward. Published on November 13, 2012 as DOI: 10.1124/mol.112.082578
This article has not been copyedited and formatted. The final version may differ from this version.

population, but not in the euploid cell population. Together, these results suggest that the novel small molecule inhibitor, obtusilactone B, preferentially targets oncogenic cells by blocking the cellular functions of BAF protein.

Discussion

Genomic DNA is attached to the nuclear envelope during interphase via the interaction of the core nuclear envelope constituents lamin and BAF (Margalit et al., 2007). The interaction between DNA and the nuclear envelope is very important for nuclear integrity and must thus be tightly regulated throughout the cell cycle. Progression of the cell cycle requires a disruption of the link between DNA and the nuclear envelope, which is achieved by VRK1-mediated BAF phosphorylation (Nichols et al., 2006). This process is very important for various cell functions; thus *Baf* is well conserved from *Drosophila melanogaster* to *Homo sapiens*.

Here, we report a small molecule inhibitor, obtusilactone B, that targets BAF and inhibits VRK1-mediated phosphorylation. Obtusilactone B interacts with BAF specifically and suppresses subsequent VRK1-mediated BAF phosphorylation. Specific binding of obtusilactone B to cellular BAF causes an aberrant interaction between DNA and the nuclear envelope during the mitotic phase. We also demonstrated that obtusilactone B targets tumor cells and selectively kills aneuploid cells *in vitro*.

However, more detailed molecular mechanistic studies should be performed to conclude that obtusilactone B has genuine specificity for cancer cells. Such studies could include a systemic approach to phosphor-profiling of BAF protein in various cancer tissues. Additional evidence including animal experiment should also be obtained.

Molecular Pharmacology Fast Forward. Published on November 13, 2012 as DOI: 10.1124/mol.112.082578
This article has not been copyedited and formatted. The final version may differ from this version.

The nuclear envelope has not been a primary target in anti-cancer drug development. However, like other important cellular factors, nuclear envelope constituents play major roles in the regulation of proliferative gene expression and genome integrity (Chow et al., 2012). Among the nuclear envelope constituents, lamin is a key physiological regulator, and the association of lamin dysfunction with various diseases has been frequently reported recently (Burke and Stewart, 2006; Chow et al., 2012; Gonzalez-Suarez et al., 2009). These reports suggest that effective targeting of nuclear envelope constituents awaits the advent of a novel cancer drug that targets proteins such as BAF. We posit that obtusilactone B specifically targets the core nuclear envelope constituent, BAF and blocks abnormal cell division of tumor cells by inhibiting VRK1-mediated phosphorylation of BAF. A strategy targeting the action of VRK1 toward BAF might have potential therapeutic use in BAF-related abnormalities, including various cancers.

Molecular Pharmacology Fast Forward. Published on November 13, 2012 as DOI: 10.1124/mol.112.082578
This article has not been copyedited and formatted. The final version may differ from this version.

Authorship Contributions

Participated in research design : W.Kim, KY. Choi, HS.Yoon, KT.Kim

Conducted experiments : W.Kim, HS. Kwon, HN.Lyu, KH.Lee, DY.Kim, YS. Kim

Performed data analysis : W.Kim, G. Chakraborty, H.S.Yoon, KT.Kim

Wrote or contributed to the writing of the manuscript: W.Kim, HN.Lyu, HS.Yoon, KT.Kim

References

Accelrys (2011). Discovery Studio Modeling Environment, Release 3.1. In (San Diego Accelrys Software Inc.,).

Anderson, J.E., Ma, W.W., Smith, D.L., Chang, C.J., and McLaughlin, J.L. (1992). Biologically active gamma-lactones and methylketoalkenes from Lindera benzoin. *J Nat Prod* **55**:71-83.

Bradley, C.M., Ronning, D.R., Ghirlando, R., Craigie, R., and Dyda, F. (2005). Structural basis for DNA bridging by barrier-to-autointegration factor. *Nat Struct Mol Biol* **12**:935-936.

Burke, B., and Stewart, C.L. (2006). The laminopathies: the functional architecture of the nucleus and its contribution to disease. *Annu Rev Genomics Hum Genet* **7**:369-405.

Cai, M., Huang, Y., Zheng, R., Wei, S.Q., Ghirlando, R., Lee, M.S., Craigie, R., Gronenborn, A.M., and Clore, G.M. (1998). Solution structure of the cellular factor BAF responsible for protecting retroviral DNA from autointegration. *Nat Struct Biol* **5**:903-909.

Chakraborty, G., Shin, J., Nguyen, Q.T., Harikishore, A., Baek, K., and Yoon, H.S. (2012). Solution structure of FK506-binding protein 12 from Aedes aegypti. *Proteins* **80**:2476-2481.

Choi, B.H., Kim, W., Wang, Q.C., Kim, D.C., Tan, S.N., Yong, J.W., Kim, K.T., and Yoon, H.S. (2008). Kinetin riboside preferentially induces apoptosis by modulating Bcl-2 family proteins and caspase-3 in cancer cells. *Cancer lett* **261**:37-45.

Chow, K.H., Factor, R.E., and Ullman, K.S. (2012). The nuclear envelope environment and its cancer connections. *Nat Rev Cancer* **12**:196-209.

Cragg, G.M., Grothaus, P.G., and Newman, D.J. (2009). Impact of natural products on developing new anti-cancer agents. *Chem Rev* **109**:3012-3043.

Furukawa, K., Sugiyama, S., Osouda, S., Goto, H., Inagaki, M., Horigome, T., Omata, S., McConnell, M., Fisher, P.A., and Nishida, Y. (2003). Barrier-to-autointegration factor plays crucial roles in cell cycle progression and nuclear organization in Drosophila. *J Cell Sci* **116**:3811-3823.

Gonzalez-Suarez, I., Redwood, A.B., Perkins, S.M., Vermolen, B., Lichtensztejin, D., Grotsky, D.A., Morgado-Palacin, L., Gapud, E.J., Sleckman, B.P., Sullivan, T., et al. (2009). Novel roles for A-type lamins in telomere biology and the DNA damage response pathway. The *EMBO J* **28**:2414-2427.

Gorjanacz, M., Klerkx, E.P., Galy, V., Santarella, R., Lopez-Iglesias, C., Askjaer, P., and Mattaj, I.W. (2007). Caenorhabditis elegans BAF-1 and its kinase VRK-1 participate directly in post-mitotic nuclear envelope assembly. *EMBO J* **26**:132-143.

Haraguchi, T., Koujin, T., Osakada, H., Kojidani, T., Mori, C., Masuda, H., and Hiraoka, Y. (2007). Nuclear localization of barrier-to-autointegration factor is correlated with progression

of S phase in human cells. *J Cell Sci* **120**:1967-1977.

Harris, D., and Engelman, A. (2000). Both the structure and DNA binding function of the barrier-to-autointegration factor contribute to reconstitution of HIV type 1 integration in vitro. *J Biol Chem* **275**:39671-39677.

Hiroyuki Karikome, Y.M., Yutaka Sashida (1991). A butanolide and phenolics from Machilus thunbergii. *Phytochemistry* **30**:315-319.

Kang, T.H., Park, D.Y., Choi, Y.H., Kim, K.J., Yoon, H.S., and Kim, K.T. (2007). Mitotic histone H3 phosphorylation by vaccinia-related kinase 1 in mammalian cells. *Mol Cell Biol* **27**:8533-8546.

Kang, T.H., Park, D.Y., Kim, W., and Kim, K.T. (2008). VRK1 phosphorylates CREB and mediates CCND1 expression. *J Cell Sci* **121**:3035-3041.

Karlsson, R., Michaelsson, A., and Mattsson, L. (1991). Kinetic analysis of monoclonal antibody-antigen interactions with a new biosensor based analytical system. *J Immunol Methods* **145**:229-240.

Kim, W., Chakraborty, G., Kim, S., Shin, J., Park, C.H., Jeong, M.W., Bharatham, N., Yoon, H.S., and Kim, K.T. (2012). macroH2A1 suppresses mitotic kinase VRK1 during interphase. *J Biol Chem* **287**:5278-5289.

Kuo, S.Y., Hsieh, T.J., Wang, Y.D., Lo, W.L., Hsui, Y.R., and Chen, C.Y. (2008). Cytotoxic constituents from the leaves of Cinnamomum subavenium. Chem Pharm Bull (Tokyo) **56**:97-101.

Lancaster, O.M., Cullen, C.F., and Ohkura, H. (2007). NHK-1 phosphorylates BAF to allow karyosome formation in the Drosophila oocyte nucleus. *J Cell Biol* **179**: 817-824.

Lapenna, S., and Giordano, A. (2009). Cell cycle kinases as therapeutic targets for cancer. *Nat Rev Drug Discov* **8**:547-566.

Lopez-Sanchez, I., Sanz-Garcia, M., and Lazo, P.A. (2009). Plk3 interacts with and specifically phosphorylates VRK1 in Ser342, a downstream target in a pathway that induces Golgi fragmentation. *Mol Cell Biol* **29**:1189-1201.

Margalit, A., Brachner, A., Gotzmann, J., Foisner, R., and Gruenbaum, Y. (2007). Barrier-to-autointegration factor--a BAFfling little protein. *Trends Cell Biol* **17**:202-208.

Masatake Niwa, M.I., Shosuke Yamamura (1975). The structures of c17-obtusilactone dimer and two c21-obtusilactones. *Tetrahedron Letters* **16**:4395-4398.

Nezu, J., Oku, A., Jones, M.H., and Shimane, M. (1997). Identification of two novel human putative serine/threonine kinases, VRK1 and VRK2, with structural similarity to vaccinia virus B1R kinase. *Genomics* **45**:327-331.

Nichols, R.J., Wiebe, M.S., and Traktman, P. (2006). The vaccinia-related kinases phosphorylate the N' terminus of BAF, regulating its interaction with DNA and its retention in the nucleus. *Mol Biol Cell* **17**:2451-2464.

Skoko, D., Li, M., Huang, Y., Mizuuchi, M., Cai, M., Bradley, C.M., Pease, P.J., Xiao, B., Marko, J.F., Craigie, R., et al. (2009). Barrier-to-autointegration factor (BAF) condenses DNA by looping. *Proc Natl Acad Sci U S A* **106**:16610-16615.

Suzuki, Y., Ogawa, K., and Koyanagi, Y. (2010). Functional disruption of the moloney murine leukemia virus preintegration complex by vaccinia-related kinases. *J Biol Chem* **285**:24032-24043.

Valbuena, A., Lopez-Sanchez, I., and Lazo, P.A. (2008). Human VRK1 is an early response gene and its loss causes a block in cell cycle progression. *PLoS One* **3**:e1642.

Verdonk, M.L., Cole, J.C., Hartshorn, M.J., Murray, C.W., and Taylor, R.D. (2003). Improved protein-ligand docking using GOLD. *Proteins* **52**:609-623.

Vlcek, S., Dechat, T., and Foisner, R. (2001). Nuclear envelope and nuclear matrix: interactions and dynamics. *Cell Mol Life Sci* **58**:1758-1765.

Footnotes

This work was supported by grants from the National Research Foundation of Korea (NRF) [Nos. 20110027957, 20110031234, 20120005830, 20110031517], the Brain Korea 21 program, the World Class University program [R31-10105] funded by the Korean Ministry of Education, Science, and Technology (MEST), and Singapore Ministry of Education AcRF Tier 2 Grant (ARC 25/12). We thank Amaravadhi Harikishore for his help on protein ligand docking. W.K., H.-N.L., and H.-S.K. contributed equally to this work.

.

.

Molecular Pharmacology Fast Forward. Published on November 13, 2012 as DOI: 10.1124/mol.112.082578
This article has not been copyedited and formatted. The final version may differ from this version.

Figure legends

Fig. 1 Small molecule inhibitors of BAF phosphorylation

A, Crude extracts from *M.thunbergii* solubilized into indicated solvents were added to *in vitro* kinase reaction of BAF by recombinant GST-VRK1. B, Five kinds of butanolide derivatives were purified from hexane sub-fraction. Each purified compound was added into *in vitro* kinase reaction to final concentration of 100μM. Autoradiography was acquired and proteins were stained with SYPRO Ruby. C, Chemical structures of compound 1~4. #1; Obtusilactone B, **#2**; Secosubamolide A, **#3**; 2-Octadecylidene-3-hydroxy-4-methylenebutanolide, **#4**; Linderanolide

Fig. 2 Obtusilactone B suppresses VRK1-mediated phosphorylation of BAF

A, Purified butanolide derivatives from *M. thunbergii* were added into *in vitro* kinase reaction between recombinant VRK1 and BAF to final concentration of 100 μM. Autoradiography was acquired and proteins were stained with SYPRO Ruby. B, Inhibitory activity of four butanolide derivatives was assayed. The autoradiography of each compound was quantitated by densitometry. C, *In vitro* kinase assay of BAF by recombinant GST-VRK1 was performed. The kinase reaction was performed in the varying amounts of obtusilactone B ranging to 100 μM. D-E, *In vitro* kinase assay of histone H3 and casein by recombinant GST-VRK1 were performed. Autoradiography was acquired and proteins were stained with SYPRO Ruby or Coomassie Brilliant Blue.

Fig. 3 Obtusilactone B specifically interacts with BAF

A, A plot of average chemical shift perturbations versus amino acid residues of BAF protein on addition of obtusilactone B in a 1:1 molar ratio. B, Mapping of the chemical shift

Molecular Pharmacology Fast Forward. Published on November 13, 2012 as DOI: 10.1124/mol.112.082578
This article has not been copyedited and formatted. The final version may differ from this version.

perturbations on BAF (PDB ID 2BZF) protein. The interacting residues (shown in yellow), are close to DNA binding region of BAF. C-D, Molecular docking analyses of the butanolide derivatives with BAF protein. Interaction of obtusilactone B with modeled BAF protein was shown in yellow sticks and 2-octadecylidene-3-hydroxy-4-methylenebutanolide otherwise in blue. The heterocyclic moiety in obtusilactone B is stabilized in the hydrophobic groove by hydrogen bonding with the E28 residue (shown in dashed lines) and hydrophobic contacts with V20, G25, I26, V29, L30, G31 and K32 (shown in dotted lines) residues while 2-octadecylidene-3-hydroxy-4-methylenebutanolide the same moiety lacks these interactions.

Fig. 4 SPR evidence for the interaction of obtusilactone B with BAF

A, Sensorgram overlays for the binding of obtusilactone B (red) and 2-octadecylidene-3-hydroxy-4-methylenebutanolide (blue) to BAF protein immobilized on a CMDH gold sensor chip. Shown are the binding responses (arbitrary unit) of each analyte injected at 2, 4, and 8μM over the surface. B, Obtusilactone B conjugated with FPR552 was separated by thin layer chromatography of silica gel developed with solvent system acetonitrile/water (1:2). C, A549 cells were transfected with EGFP-tagged BAF for 12 hours. After fixation, FPR552-conjugated obtusilactone B was treated for 30 minutes.

Fig. 5 Physiological perturbations induced by obtusilactone B treatment

A, A549 cells were treated with 10 μM of obtusilactone B for 72 hours. Anti-lamin A/C antibody was applied and visualized by Alexa-488 dye. DNA was also visualized by Hoechst 33342. B, HEK293A cells were transfected with red fluorescent protein-VRK1 and EGFP - BAF. After 72 hours treatment of 10 μM of obtusilactone B, fluorescent images were captured. C-D, A549 cells were treated with 25 μM of obtusilactone B for 24 hours after transfection with EGFP or EGFP-BAF. Nuclear DNAs were stained with propidium iodide,

and flow cytometric analyses were performed.

Fig. 6 Anti-cancer activity of obtusilactone B

A, A549 cells were treated with indicated amount of obtusilactone B and 2-octadecylidene-3-hydroxy-4-methylenebutanolide. After 24 hours, cell viability was assessed by measuring its activity to metabolize MTT. B, HeLa cells were treated with indicated amount of obtusilactone B and 2-octadecylidene-3-hydroxy-4-methylenebutanolide. After 24 hours, cell viability was assessed by measuring its activity to metabolize MTT. C, Mouse embryonic fibroblast derived from C57BL/6 mouse and B16F10 cells were treated with indicated amount of obtusilactone B. After 24 hours, cell viability was assessed by measuring its activity to metabolize MTT. D, F9 mice teratocarcinoma cells were treated with indicated amount of obtusilactone B. Time-laps images of live cells were acquired and confluency was assessed from Incucyte software. Arrow indicates the addition of obtusilatone B. E, A549 cells were treated with 10 μM of obtusilactone B for 72 hours. DNA was stained by propidium iodide, and flow cytometric analysis was performed. Aneuploid cell population which contains DNA content more than 4N is marked.

Molecular Pharmacology Fast Forward. Published on November 13, 2012 as DOI: 10.1124/mol.112.082578
This article has not been copyedited and formatted. The final version may differ from this version.

Table 1. Binding constants between BAF and Pbtusilactone B / 2-Octadecylidene-3-hydroxy-4-methylenebutanolide

	Ka($M^{-1}S^{-1}$)	**Kd(S^{-1})**	**KD**
Obsutilactone B	$1.14 \times 10^4 \pm 0.06$	0.0158 ± 0.0004	1.39 ± 0.08 μM
2-Octadecylidene-3-hydroxy-4-methylenebutanolide	$3.0 \times 10^3 \pm 0.3$	0.0366 ± 0.0007	12 ± 1 μM

Figure 1

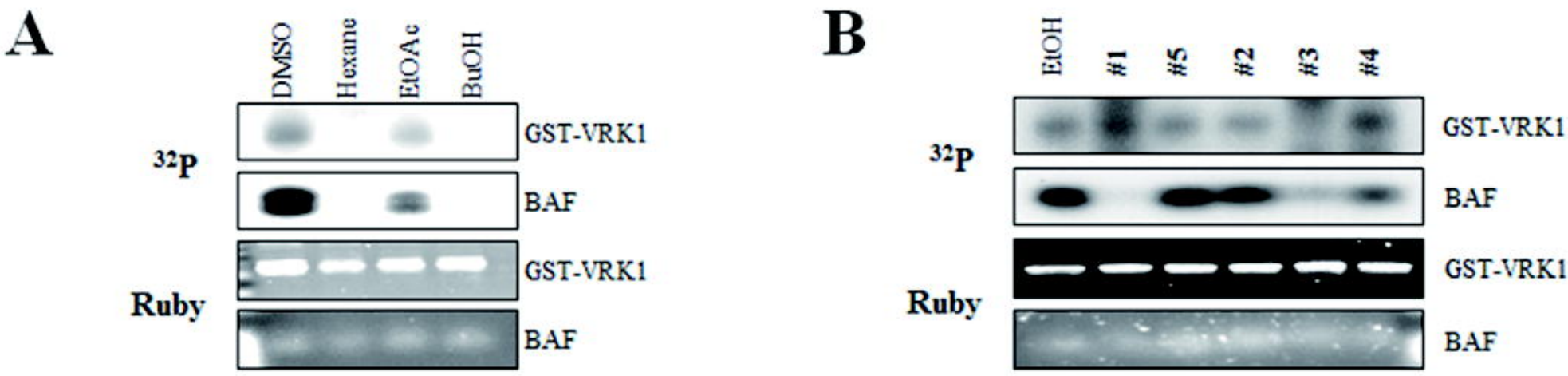
A
DMSO
Hexane
EtOAc
BuOH
32P
GST-VRK1
BAF
Ruby
GST-VRK1
BAF
B
EtOH
#1
#5
#2
#3
#4
32P
GST-VRK1
BAF
Ruby
GST-VRK1
BAF

C

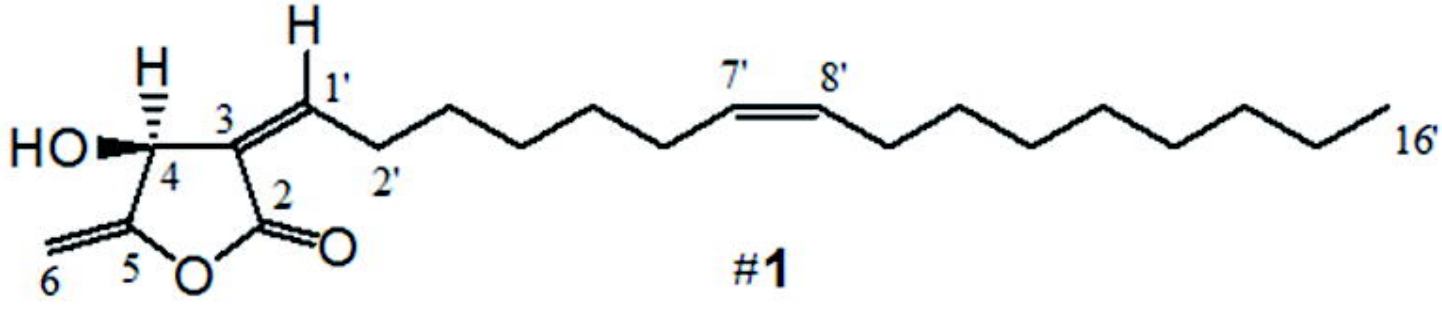
H
H
HO
1'
3
4
2
2'
7'
8'
16'
6
5
O
O
#1

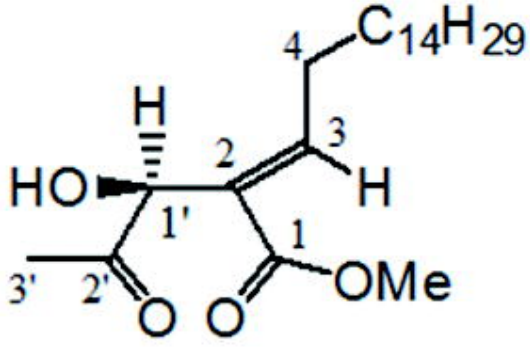
4
C14H29
H
HO
2
3
H
1'
1
3'
2'
O
O
OMe
#2

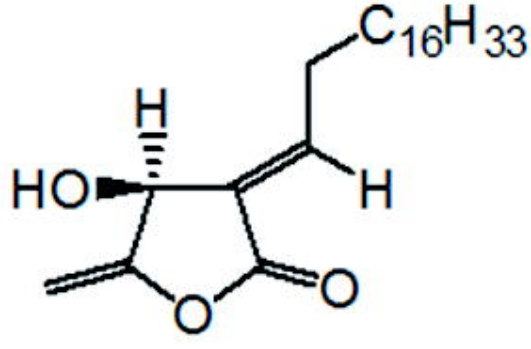
C16H33
H
HO
H
O
O
#3

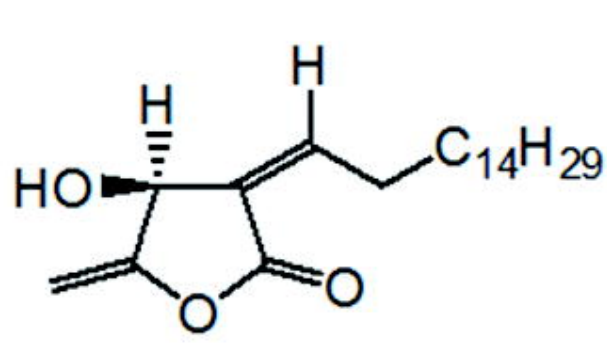
H
H
C14H29
HO
O
O
#4

Figure 2

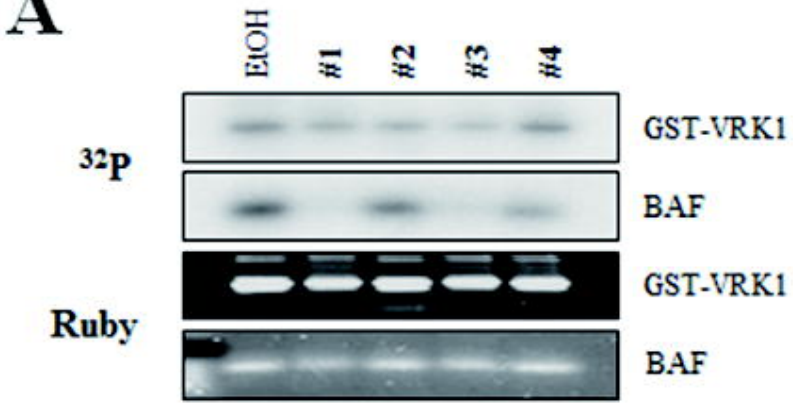
A
EtOH
#1
#2
#3
#4
32P
GST-VRK1
BAF
Ruby
GST-VRK1
BAF

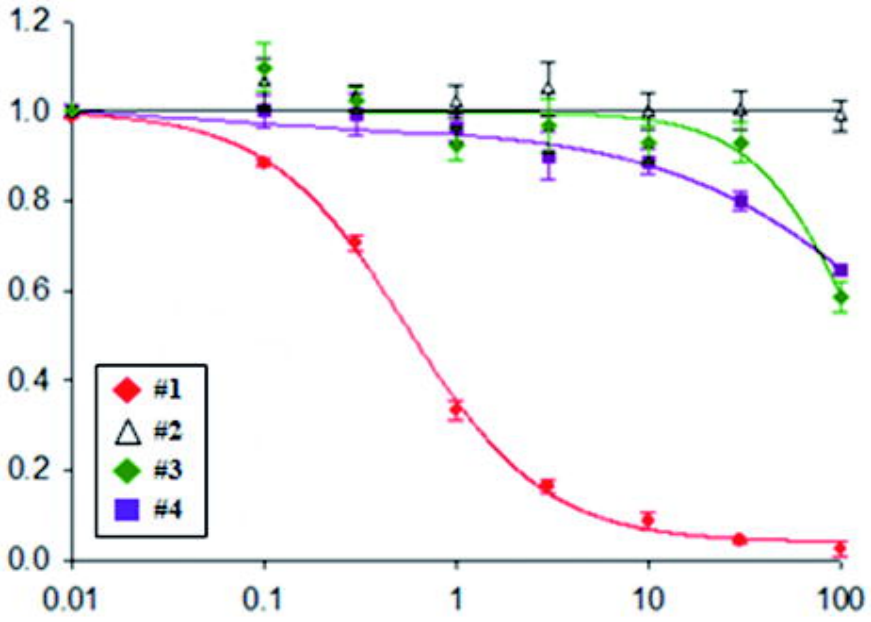
B
1.2
1.0
0.8
0.6
0.4
0.2
0.0
0.01
0.1
1
10
100
#1
#2
#3
#4

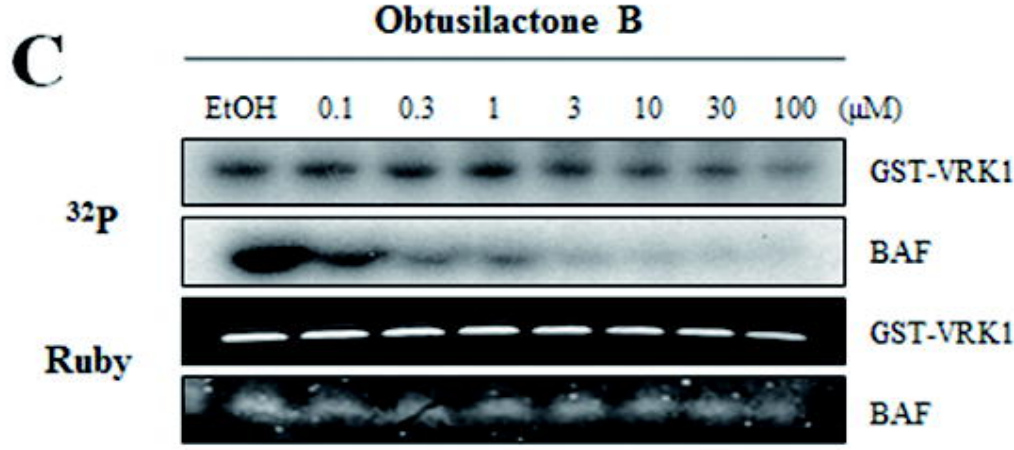
C
Obtusilactone B
EtOH
0.1
0.3
1
3
10
30
100
(μM)
32P
GST-VRK1
BAF
Ruby
GST-VRK1
BAF

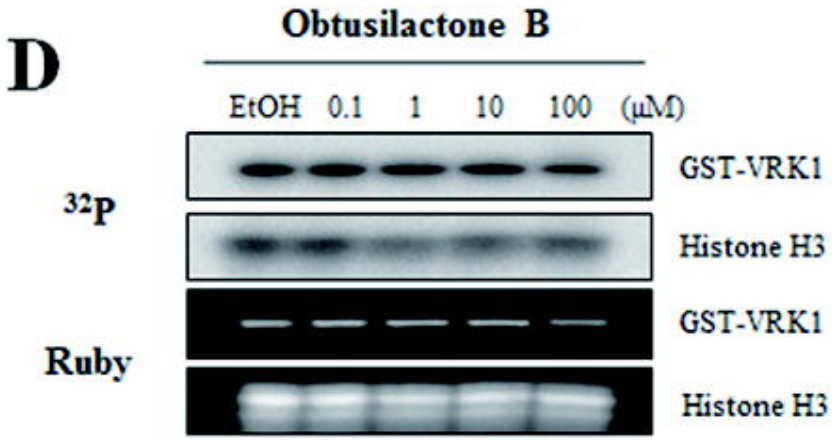
D
Obtusilactone B
EtOH
0.1
1
10
100
(μM)
32P
GST-VRK1
Histone H3
Ruby
GST-VRK1
Histone H3

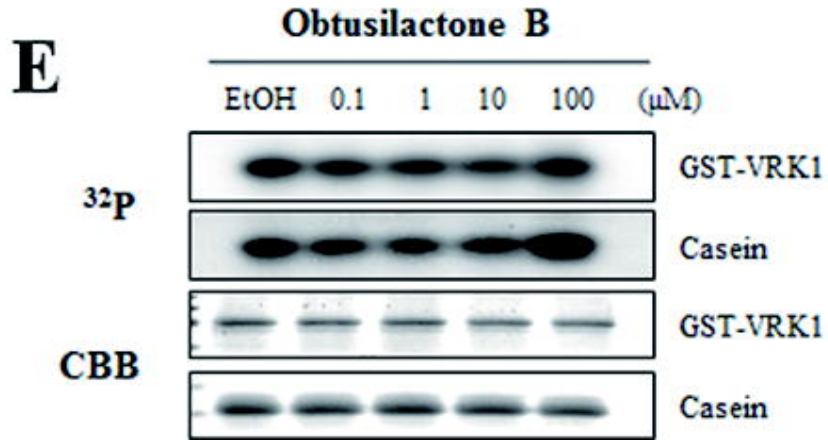
E
Obtusilactone B
EtOH
0.1
1
10
100
(μM)
32P
GST-VRK1
Casein
CBB
GST-VRK1
Casein

Figure 3

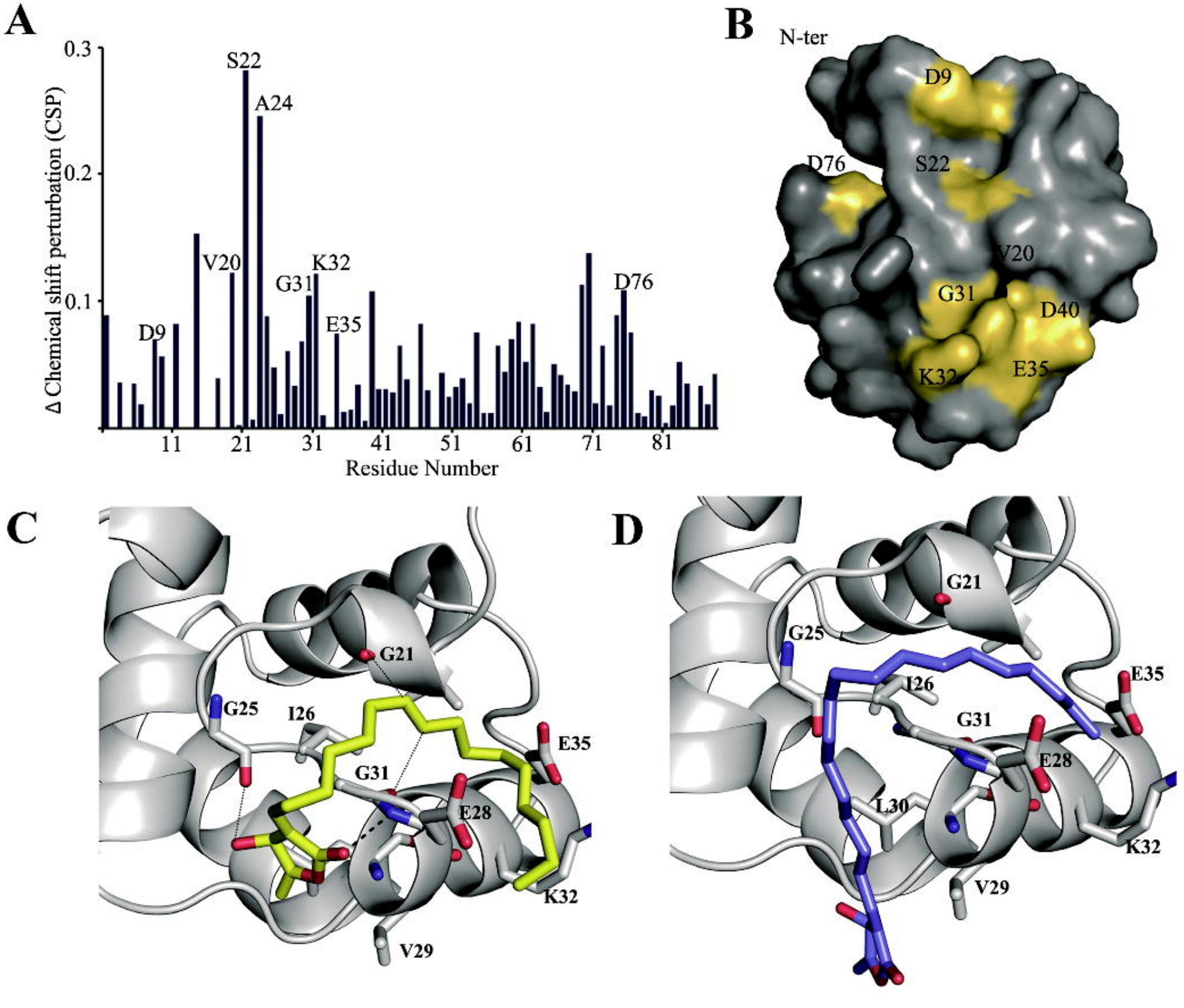
A
0.3
0.2
0.1
Δ Chemical shift perturbation (CSP)
S22
A24
V20
K32
G31
D76
D9
E35
11
21
31
41
51
61
71
81
Residue Number
B
N-ter
D9
D76
S22
V20
G31
D40
K32
E35
C
G21
G25
I26
E35
G31
E28
K32
V29
D
G21
G25
I26
E35
G31
E28
L30
K32
V29

Figure 4

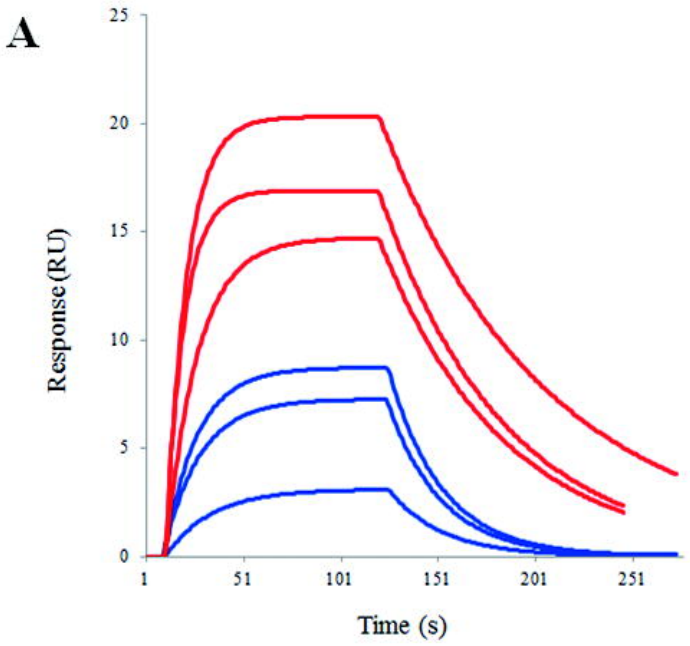
A
25
20
15
10
5
0
Response (RU)
1
51
101
151
201
251
Time (s)

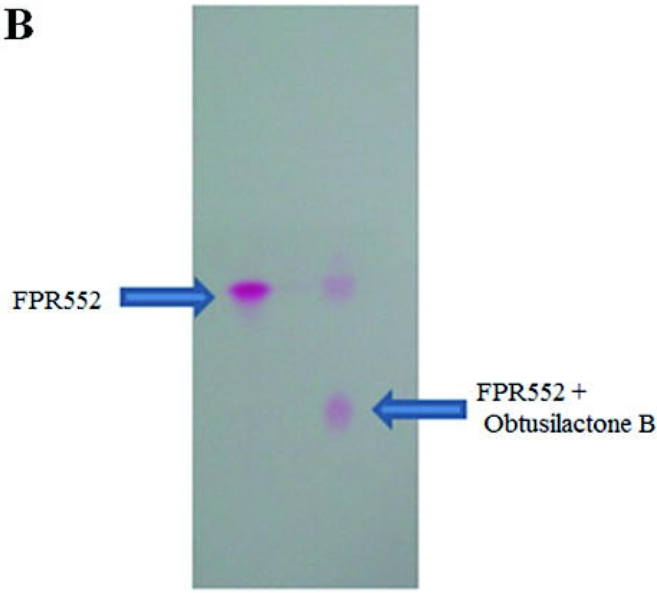
B
FPR552
FPR552 +
Obtusilactone B

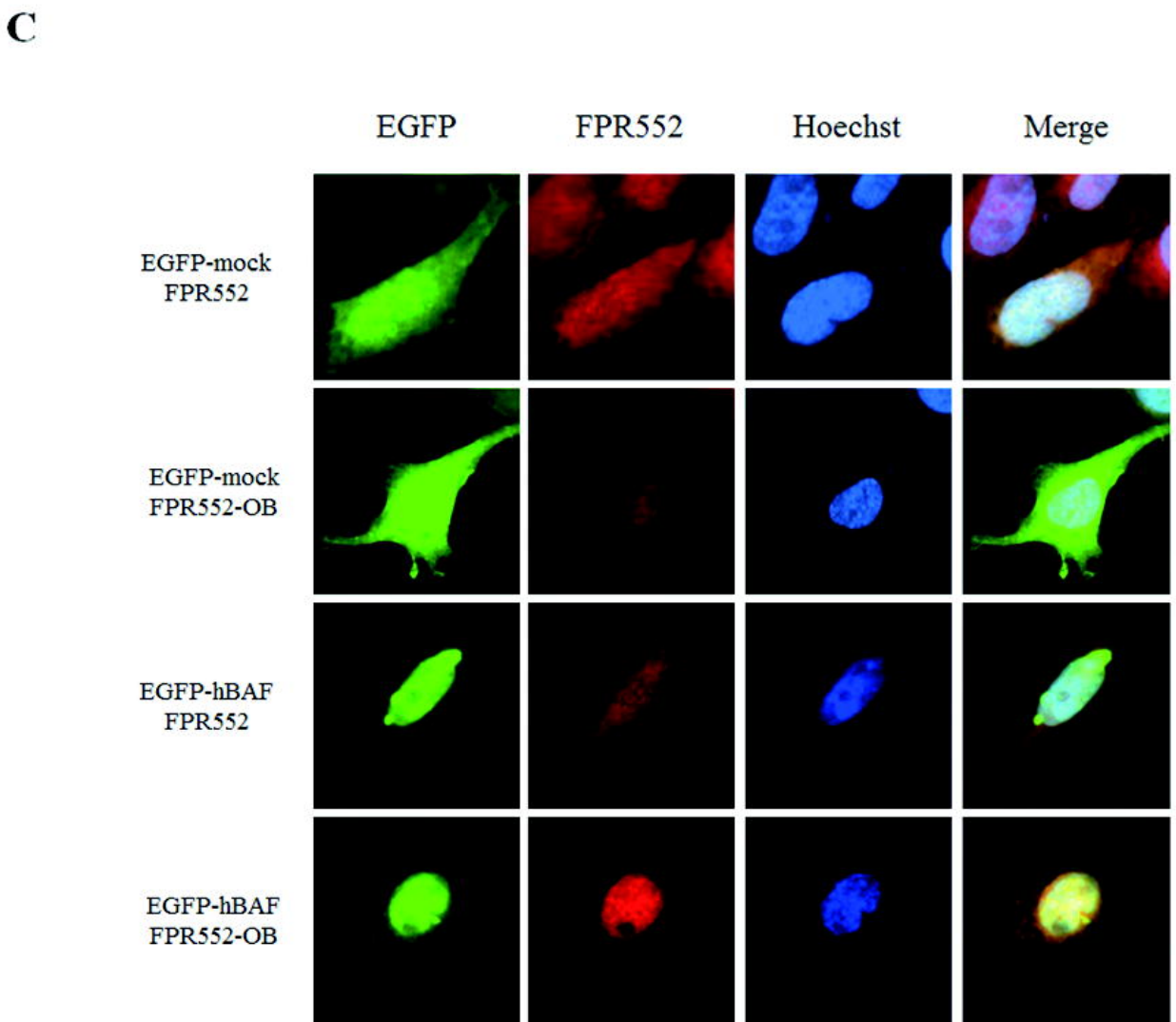
C
EGFP
FPR552
Hoechst
Merge
EGFP-mock
FPR552
EGFP-mock
FPR552-OB
EGFP-hBAF
FPR552
EGFP-hBAF
FPR552-OB

Figure 5

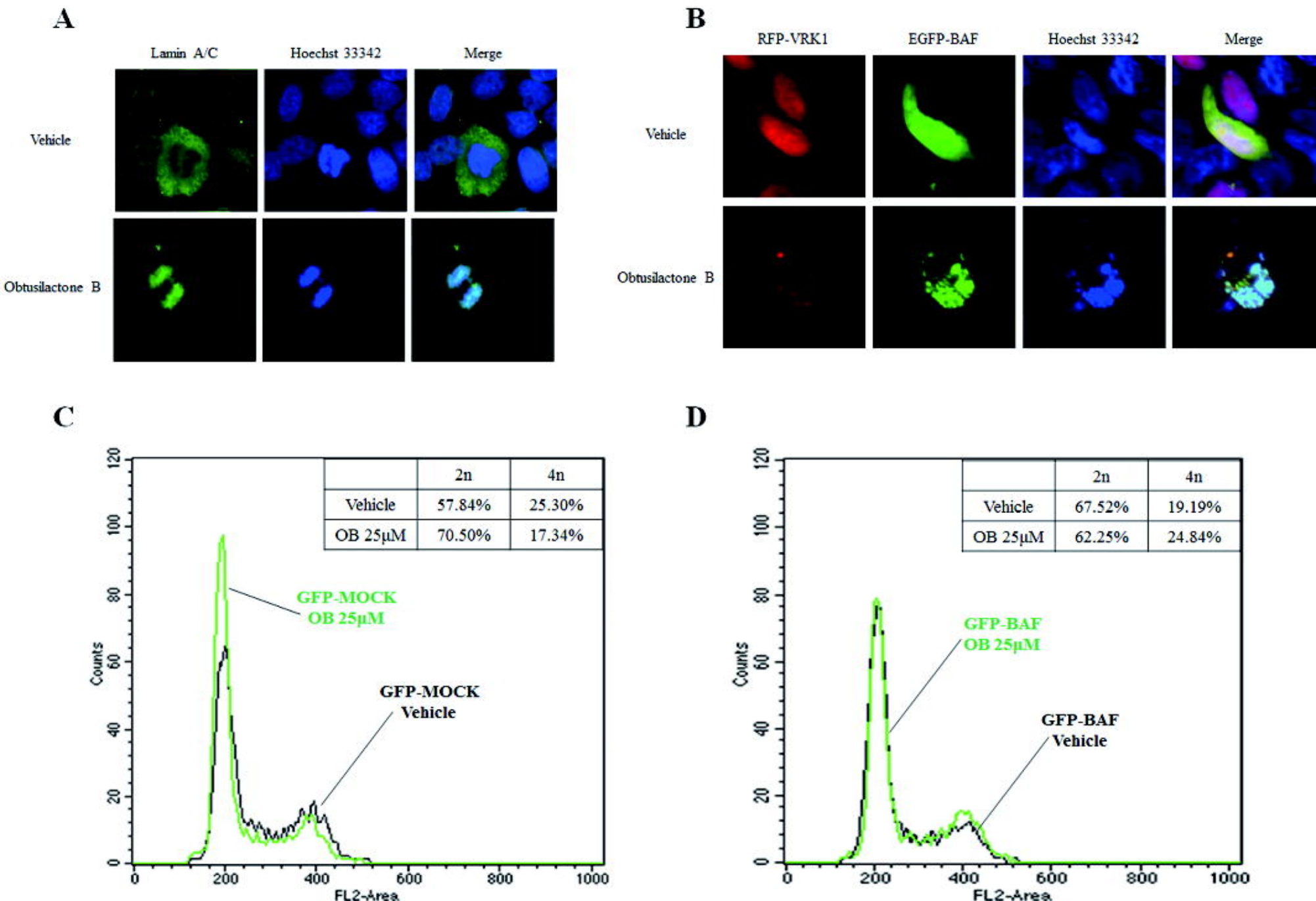
A
Lamin A/C
Hoechst 33342
Merge
Vehicle
Obtusilactone B
B
RFP-VRK1
EGFP-BAF
Hoechst 33342
Merge
Vehicle
Obtusilactone B
C
2n
4n
Vehicle
57.84%
25.30%
OB 25μM
70.50%
17.34%
GFP-MOCK
OB 25μM
GFP-MOCK
Vehicle
Counts
FL2-Area
D
2n
4n
Vehicle
67.52%
19.19%
OB 25μM
62.25%
24.84%
GFP-BAF
OB 25μM
GFP-BAF
Vehicle
Counts
FL2-Area

Figure 6

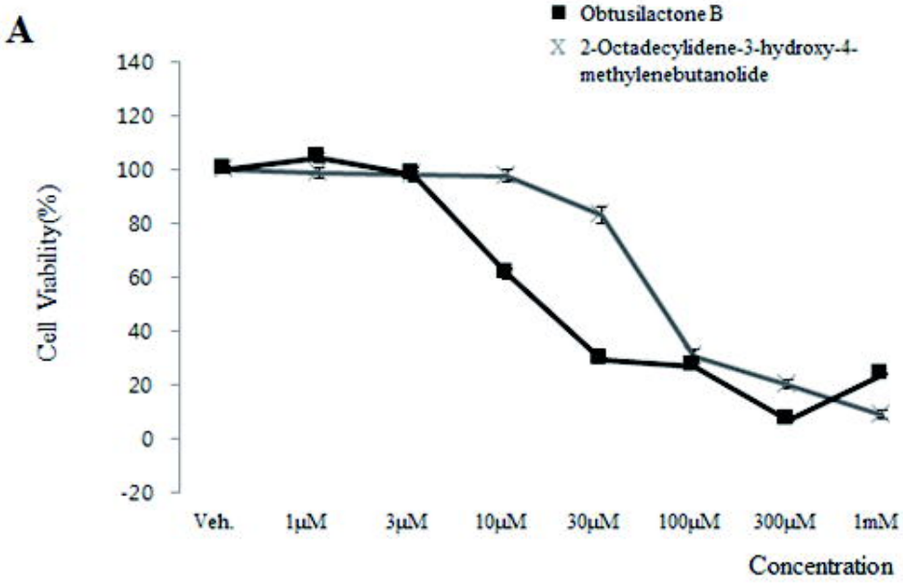
A
Obtusilactone B
2-Octadecylidene-3-hydroxy-4-methylenebutanolide
Cell Viability(%)
140
120
100
80
60
40
20
0
-20
Veh.
1μM
3μM
10μM
30μM
100μM
300μM
1mM
Concentration

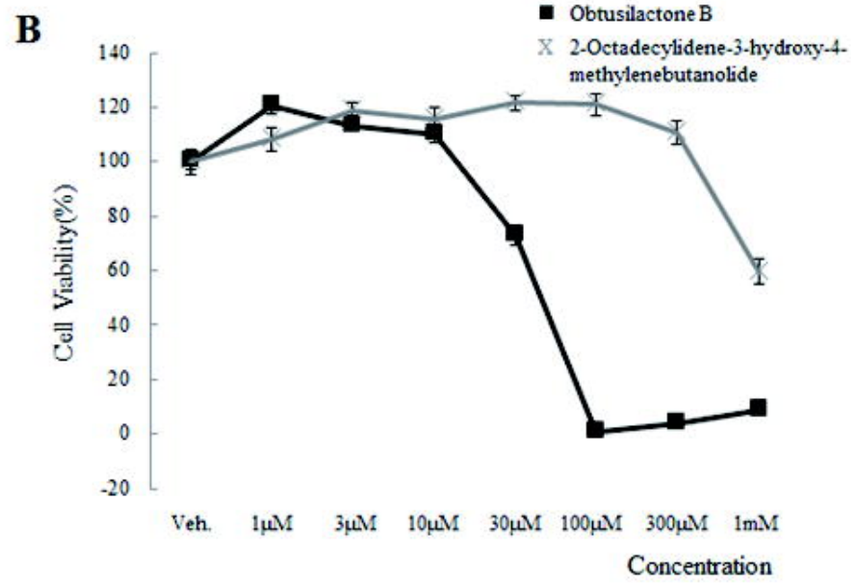
B
Obtusilactone B
2-Octadecylidene-3-hydroxy-4-methylenebutanolide
Cell Viability(%)
140
120
100
80
60
40
20
0
-20
Veh.
1μM
3μM
10μM
30μM
100μM
300μM
1mM
Concentration

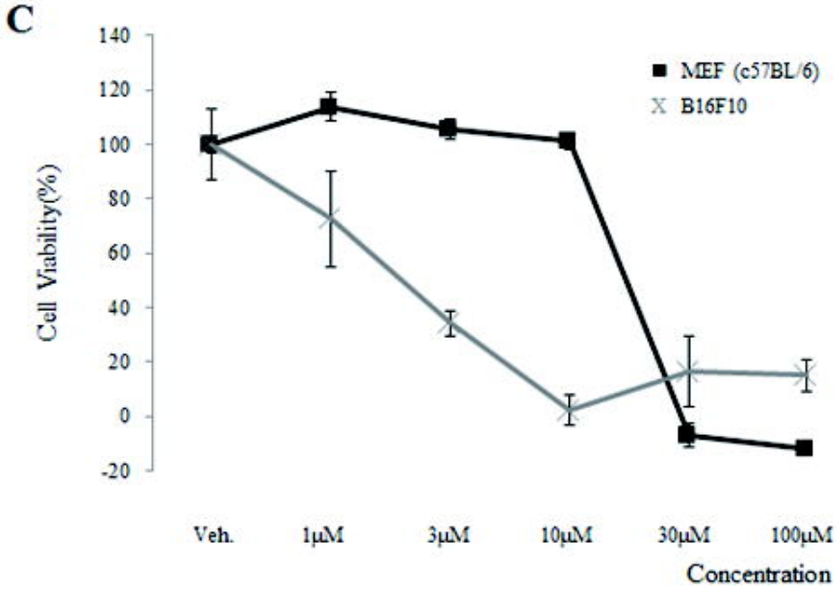
C
MEF (c57BL/6)
B16F10
Cell Viability(%)
140
120
100
80
60
40
20
0
-20
Veh.
1μM
3μM
10μM
30μM
100μM
Concentration

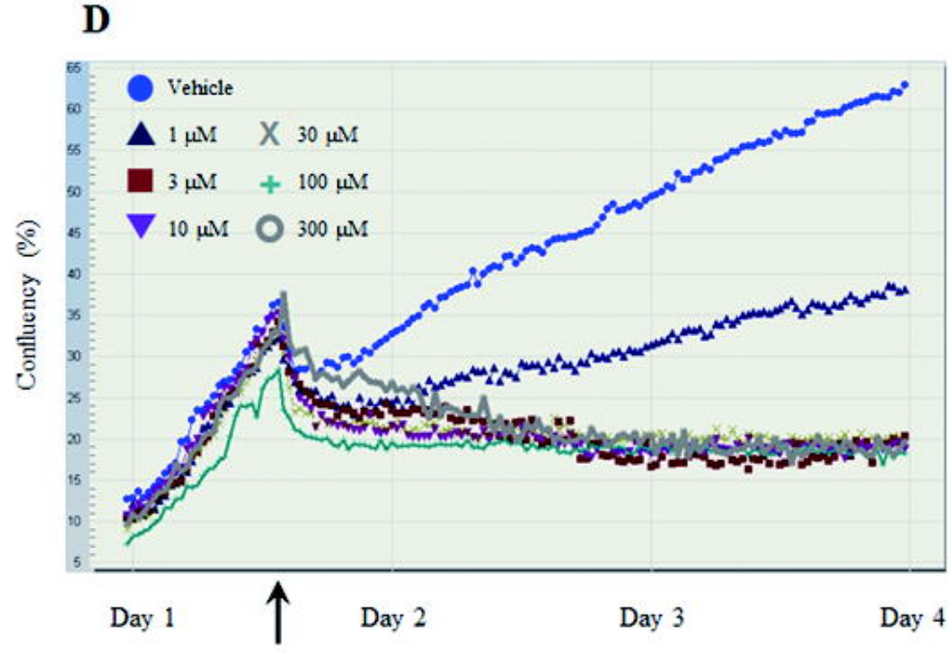
D
Vehicle
1 μM
3 μM
10 μM
30 μM
100 μM
300 μM
Confluency (%)
Day 1
Day 2
Day 3
Day 4

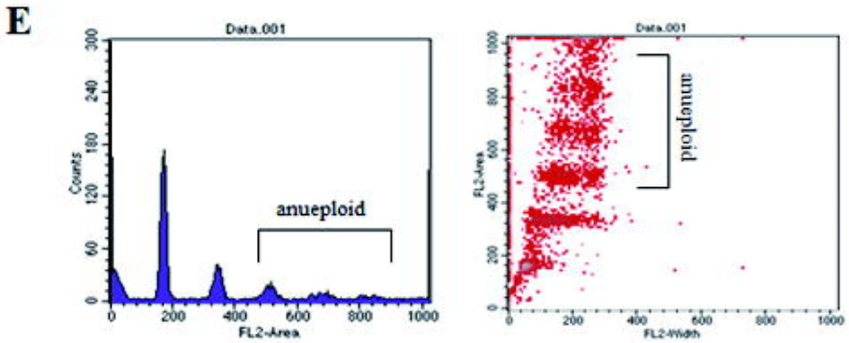
E
Data.001
anueploid
Counts
FL2-Area
Data.001
anueploid
FL2-Area
FL2-Width

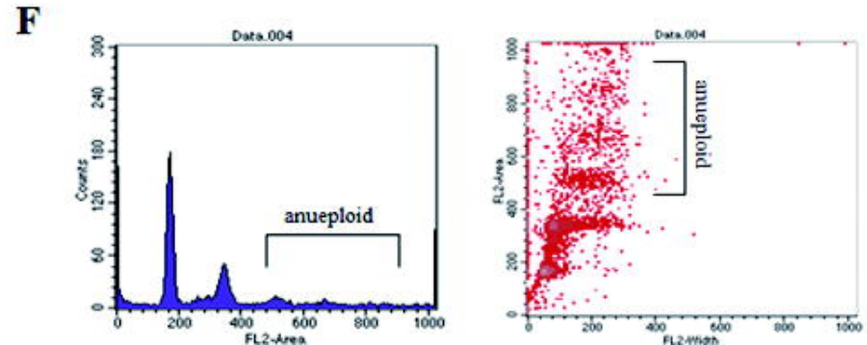
F
Data.004
anueploid
Counts
FL2-Area
Data.004
anueploid
FL2-Area
FL2-Width

Obtusilactone B from *Machilus thunbergii* targets barrier-to-autointegration factor to treat cancer

Wanil Kim, Ha-Na Lyu, Hyun-Sook Kwon, Ye Seul Kim, Kyung-Ha Lee, Do-Yeon Kim, Goutam Chakraborty, Kwan Yong Choi, Ho Sup Yoon, Kyong-Tai Kim

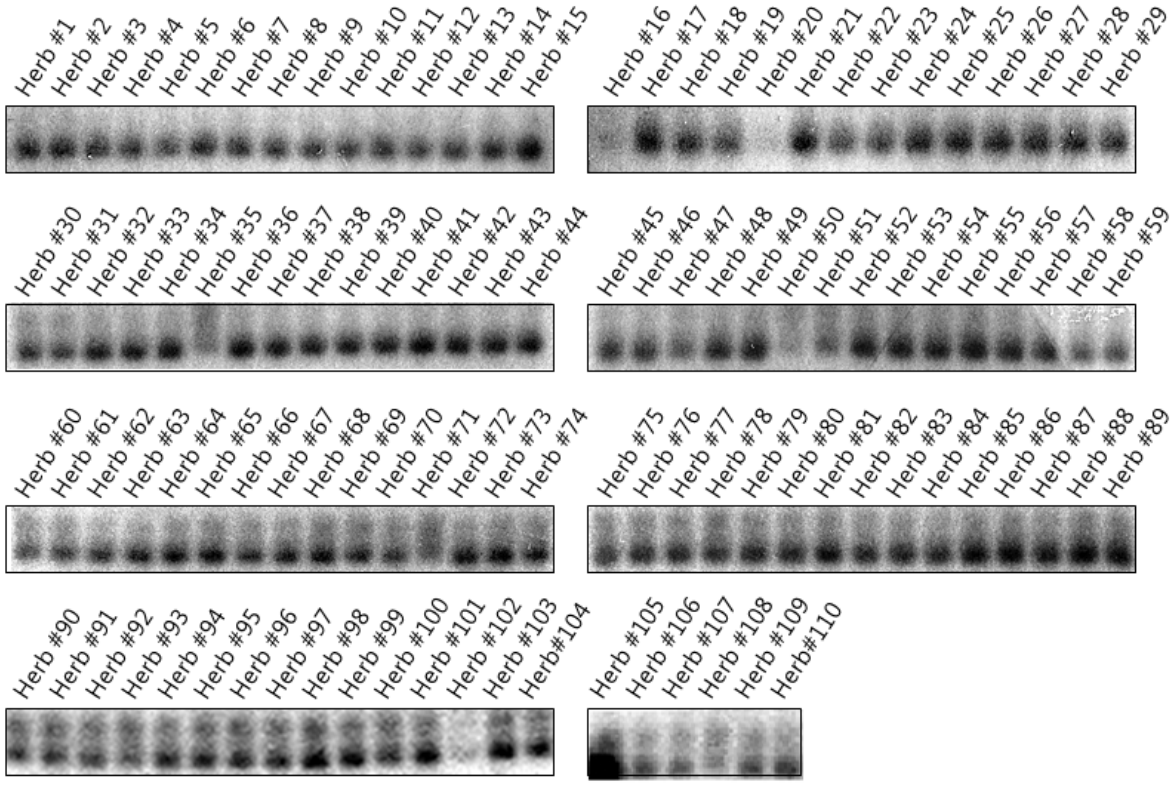

Supplemental Figure 1. Screening of inhibitors of VRK1 auto-phosphorylation from natural herb extract library. Herb extracts library was prepared by methanol-based crude extraction of various Korean traditional natural herbs. Each extract was added into *in vitro* kinase reaction of GST-VRK1 protein. Extracts from Herb #20, Herb # 35, Herb #50, Herb #71, and Herb #102 significantly reduced the auto-phosphorylation of VRK1 protein. Extract #35 is derived from *Machilus thunbergii* and further analyzed in this study.

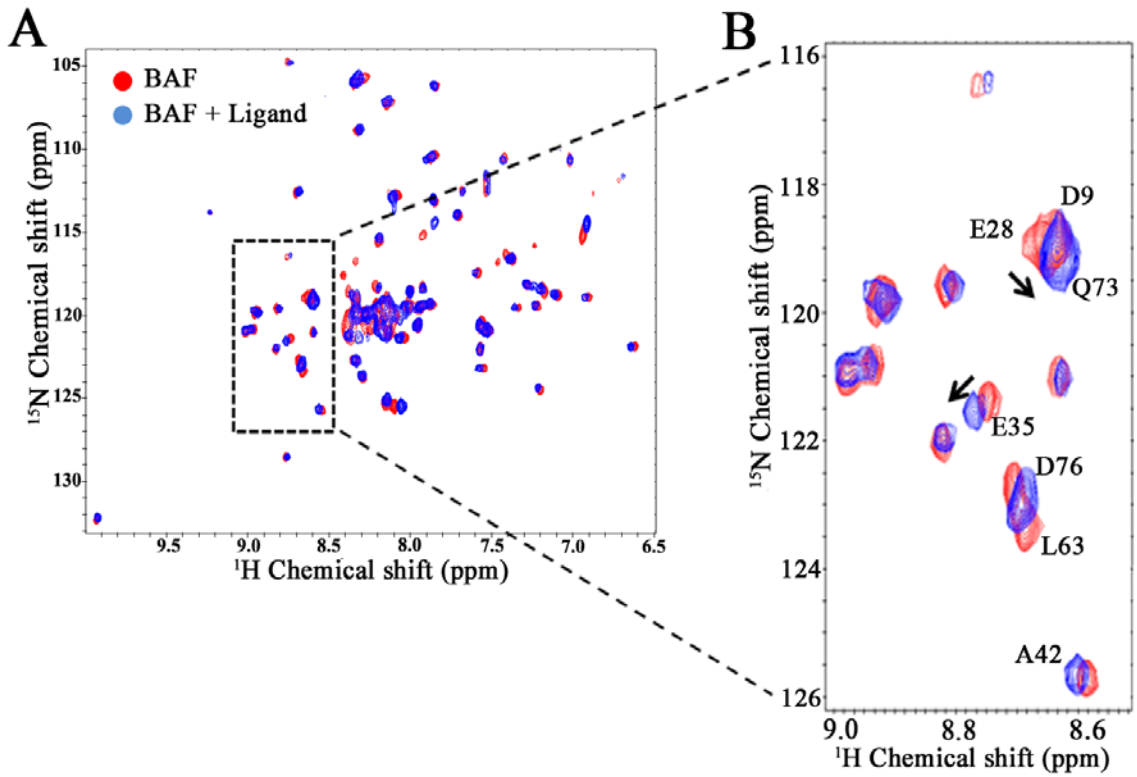

Supplemental Figure 2. (A) An overlay of the heteronuclear single quantum coherence spectra of free BAF and obtusilactone B (1:1 molar ratio) showing the chemical shift perturbations. The titration was also performed with higher dose of the drug 1:2, 1:5 doses in which saturation was observed. (B) An inset of the spectrum showing some of the interacting residues. Section of residues showing notable chemical shift perturbations are indicated by arrowhead.

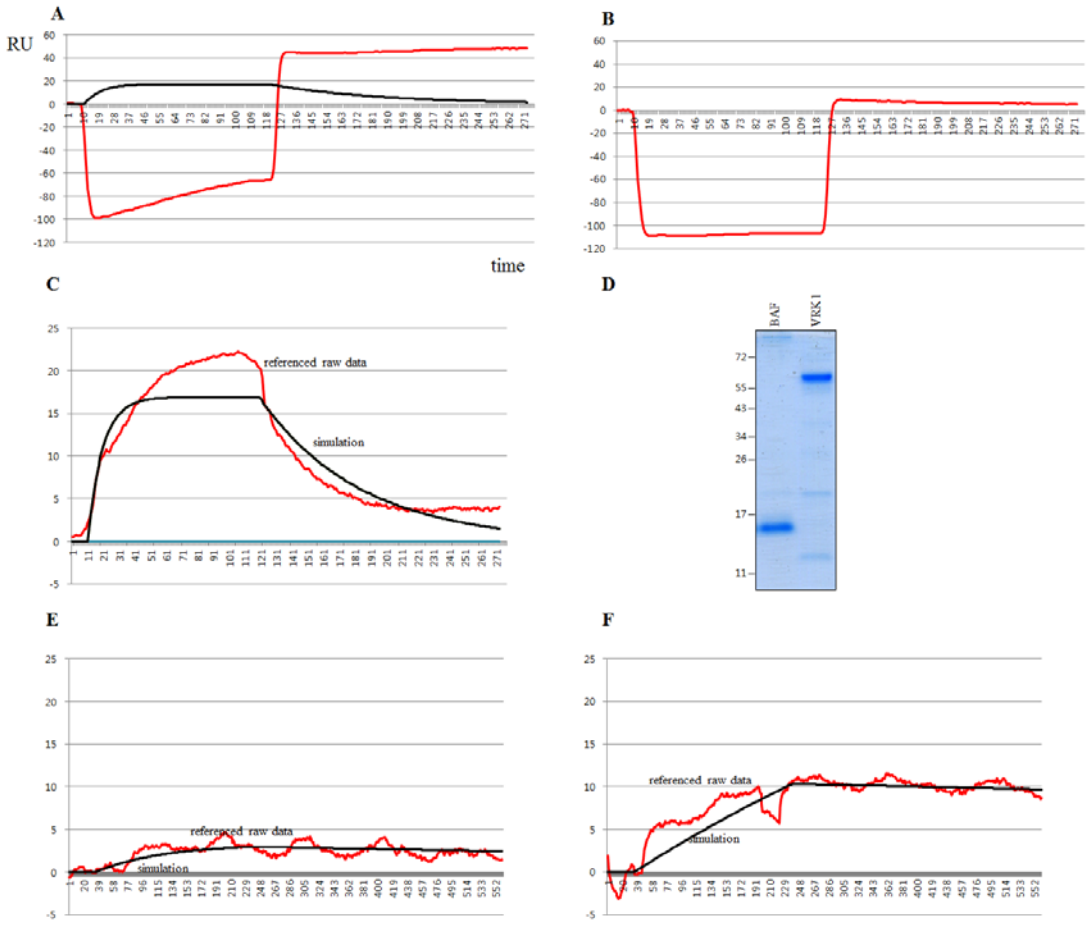

Supplemental Figure 3. Surface plasmon resonance analysis between ligand proteins and analytes. (A) Response of coated BAF protein to the flow of 8μM obtusilactone B at an analytic flow cell. (B) Response at a control flow cell which is analyzed concomitantly with the analytic flow cell. (C) Acquired response of BAF protein to 8μM obtusilactone B, which is combined from the responses of the analytic flow cell and the control flow cell. (D) 6 histidine-tagged bacterial recombinant BAF and VRK1 proteins, which are used to coat the gold chip. (E) Response of coated VRK1 protein to the flow of 8μM obtusilactone B. (F) Response of coated VRK1 protein to the flow of 8μM 2-octadecylidene-3-hydroxy-4-methylenebutanolide. Red dash shows referenced raw data; black dash shows simulated result.